EUROPEAN ORGANIZATION FOR NUCLEAR RESEARCH

CERN–SPSC–2004–018
SPSC–M–717
24 June, 2004

Status report of the HARP experiment July 2004

Abstract

The current status of the HARP experiment is described, emphasising the developments since the previous status report, which was presented in August 2003. A preliminary analysis to measure pion production for the K2K experiment with the forward spectrometer has been presented at the Rencontre de Moriond and subsequent conferences. High efficiency has been achieved for the tracking in the forward spectrometer with a good momentum resolution. The PID is capable of cleanly separating electrons, pions and protons in the relevant momentum range.

A short description of the developments needed to finish the pion production analysis for the K2K experiment is given.

The work on the calibration of the TPC is nearly finished and has been presented at the Siena conference. The results of the TPC-calibration campaign performed in 2003 with cosmic rays have permitted a better understanding of the energy-deposition response, momentum resolution and the electrostatic distortions. An algorithm to correct for the cross-talk is operational. A full simulation describing the performance of the TPC is available.

1 Introduction

The HARP experiment was designed to perform a systematic and precise study of hadron production for beam momenta between 2 and 15 GeV/c , for target nuclei ranging from hydrogen to lead. A schematic drawing of the apparatus is shown in Fig. 1. It is a large acceptance spectrometer, with two distinct regions:

- A forward region (up to polar angles of about 250 mrad) where the main tracking devices are a set of drift chambers recuperated from the NOMAD experiment (NDC) [1], and where particle identification is possible thanks to the combination of three different detectors, a threshold Cherenkov, a time-of-flight wall (TOF) [2, 3] and a calorimeter (recuperated from CHORUS [4]) and muon identifier.
- A large-angle region, where the main tracking device and particle-id detector is a time projection chamber (TPC) [5], complemented by a set of resistive plate chamber (RPC) detectors [6].

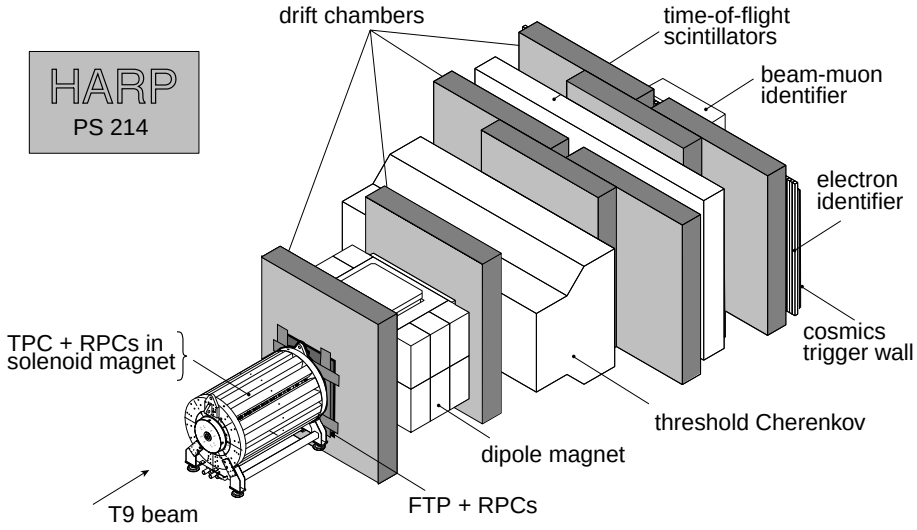

Figure 1: Schematic layout of the HARP spectrometer.

HARP physics goals are the measurement of pion yields to enable a quantitative design of the proton driver of neutrino factories and to make possible more precise calculations of the atmospheric neutrino flux. In addition, the energy-range is suitable for measuring particle yields for the prediction of neutrino fluxes for the MiniBooNE [7] and K2K [8] experiments. To this end a collaboration was set up with these groups. Beam energy settings and dedicated targets were used to provide the most relevant measurements.

This report summarises the progress of HARP since the previous status report of August 2003 [9]. In the previous report the capability of the forward detectors was demonstrated. The strategy to give priority to the analysis of the K2K-data was described and endorsed by the SPSC. Indeed, first results of the "K2K-analysis" have been presented at conferences. The proceedings of the contribution to the "Rencontre de Moriond" [10] will be attached as an appendix.

In this report the improvements achieved in the analysis following Moriond will be briefly described and the topics needed to be addressed before a first publication can be completed will be pointed out.

At the time of the previous report, more groundwork was still needed for the large angle detectors, mainly due to some difficulties discovered with the TPC hardware. The status of the characterisation of the TPC-performance will be discussed. The proceedings of the "Siena conference"[11] will be the basis for this discussion and is attached as Appendix.

The work on the software has continued to enable the handling of the large HARP data-set efficiently. The status of the definitions of the various types of "DST" will be described.

2 Forward Detectors

2.1 Status of the analysis for Moriond and recent improvements

The status of the analysis as presented at Moriond is given in the form of a reproduction of the proceedings in the Appendix.

The collaboration concentrated on the analysis of the data to measure pion production yields for the K2K experiment (*K2K analysis*). A preliminary version of the tracking and PID algorithms was used:

- Only tracks with complete information upstream and downstream of the dipole magnet were used (*type-I tracks*). Apart from the trivial decrease of statistics, this has the effect of enhancing the dependence on multi-particle correlations, and hence introduces a model-dependence in its correction. The analysis is now improved by allowing tracks where only a short segment upstream of the magnet is seen (*type-II*), or where no upstream segments and only hits are found (*type-III*). For the type-III tracks the downstream information is still sufficient to allow a consistency check with the hypothesis that the track originates from the target, and the momentum can be measured using the target-constraint. The efficiency is measured using the redundancy of the data and is well reproduced by the simulation as shown in Fig. 2. The model dependence of the efficiency correction is now expected to be small, but will be evaluated carefully in the near future.
- A PID algorithm was implemented which allows the separation of electrons, pions and protons to be performed in the full momentum range of this analysis. The new algorithm treats the hypotheses for all particle species at the same time and provides the efficiency and purity estimates. Therefore, no model is now needed to subtract proton and electron background in the pion production measurement. It uses an iterative Bayesian approach to solve the migration of particles between the different types and after a few iterations the dependence on the *prior* is removed. Results of this algorithm are shown in the following sections.

3 Results presented at the neutrino2004 conference

With these new algorithms in place, more reliable results were presented mid June at the Neutrino 2004 conference. We summarise these results by showing the particle ID corrections, the overall tracking efficiencies and the yields.

The yield for each type of track must be corrected by the pion efficiency and purity. These quantities are computed with beam particles for which a very strong redundant PID is provided

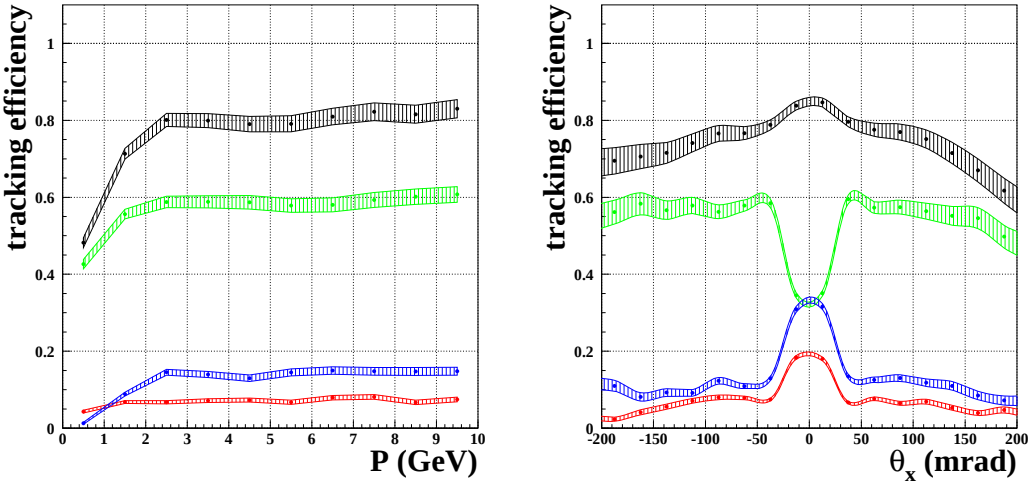

Figure 2: Total tracking efficiency as a function of p (left) and θ_x (right) for simulated data. The total efficiency is the sum of the normalized efficiency for each type. Upper curve: total, and then respectively type-I, type-II, type-III.

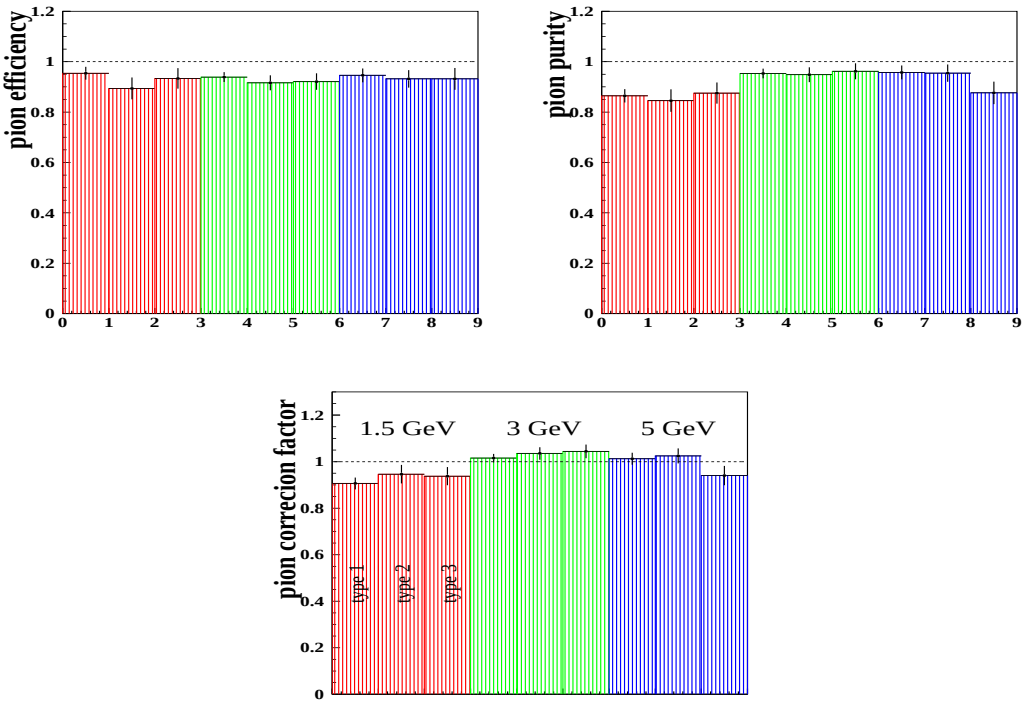

Figure 3: Pion efficiency, purity and correction factor for the three track-types and for 1.5, 3 and 5 GeV/c respectively. The organisation of the plots is indicated on the lower panel.

by the beam detectors. The PID efficiency and purity are defined as follows:

$$\varepsilon_i^{\pi-(t)} = \frac{N_i^{\pi-true-obs}}{N_i^{\pi-true}} = \frac{tracked\ true\ pions\ identified\ as\ such}{tracked\ true\ pions} \tag{1}$$

$$\eta_i^{\pi-(t)} = \frac{N_i^{\pi-true-obs}}{N_i^{\pi-obs}} = \frac{tracked\ true\ pions\ identified\ as\ such}{tracked\ particles\ identified\ as\ pions} \tag{2}$$

The pion correction factor for each track type is $\frac{\eta_i^{\pi-(t)}}{\varepsilon_i^{\pi-(t)}}$. Fig. 3 shows the pion efficiency, purity and correction factor, for the three track types, for 1.5, 3 and 5 GeV/c beam particles, respectively.

In order to ensure good efficiency the following fiducial cuts were applied: $p > 0.2$ GeV/c, $|\theta_y| < 50$ mrad, $25 < |\theta_x| < 200$ mrad. The latter cut at small angles removes the region affected by the bias in the trigger and by the saturation effects in the first drift-chamber module. The cut in $|\theta_y|$ corresponds to the vertical aperture of the dipole magnet. These cuts are applied for all efficiency calculations, see Fig. 4. The pion yield within the fiducial cut region is also displayed in this figure.

A number of improvements are being implemented to finalise the K2K-analysis.

- The absolute normalisation is not strictly needed for K2K, since the experiment uses a ratio of far and near detector event-rate. However, in order to make the data of general use an absolute normalisation will be determined. The normalisation is relatively straightforward and is based on counting incident protons using the *minimum bias* trigger events.
- Resolution effects have to be corrected using an unfolding method. An approach based on the work of D'Agostini[12] is being used. Owing to the good resolution, no difficulties are expected. This method has already been tested for a preliminary analysis [13].
- A small amount of background is still present in the data. In the forward analysis, tracks originating from the end-plug of the inner field-cage of the TPC cannot be distinguished from tracks originating in the target. A sufficient number of empty-target runs is available to perform a subtraction. These data were taken at each change of setting, thus sampling the detector performance at regular intervals. The normalisation is needed for this subtraction.
- A full analysis of the systematic errors of this measurement is being performed.

3.1 Improved TOF resolution for beam particles

A better time resolution of the TOF-detectors in the beam is now achieved by carrying out all time-slewing corrections. After identification of the particle type in the beam the combination of the knowledge of the mass of the particle and the beam momentum makes it possible to use the weighted average time of the beam TOF detectors to use as reference for the time measurement in the TOF wall. The achieved resolution of this reference time is 70 ps.

The beam time-of-flight system is made of two scintillator planes (ToFA/B) and a Target Defining Scintillator (TDS). These three devices in combination provide a means for determining the

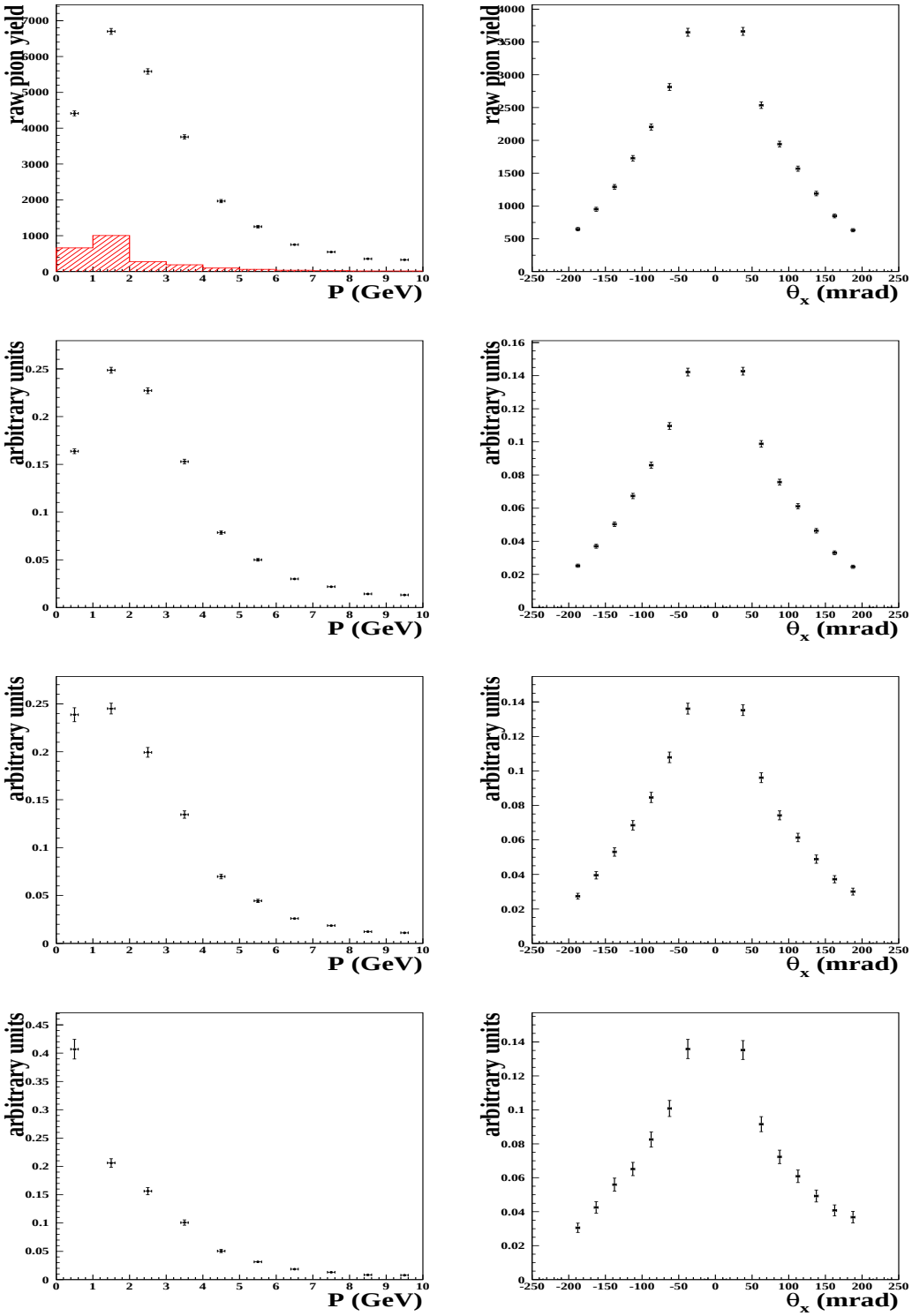

Figure 4: Results of this analysis in terms of pion yields as function of momentum and angle. The four rows show from top to bottom: raw pion yield, and the yield after the application of the pion PID-correction factor, efficiency correction and acceptance correction, respectively. The filled histogram in the left upper panel corresponds to the combined proton and electron background. This background is corrected for in the subsequent rows with the method described in the text. All distributions are for the region $p > 0.2$ GeV/c, $|\theta_y| < 50$ mrad, $25 < |\theta_x| < 200$ mrad.

Run	Momentum	σ_A (ps)	σ_B (ps)	σ_{TDS} (ps)	σ_{t_0}
19130	**1.5 GeV/c**	109.5	136.7	138.2	**72.7 ps**
14180	**3.0 GeV/c**	114.4	130.9	135.8	**72.8 ps**
14425	**5.0 GeV/c**	108.3	130.8	141.7	**71.9 ps**
17900	**8.9 GeV/c**	115.4	116.7	138.5	**70.6 ps**
18263	**12.9 GeV/c**	108.2	118.0	128.4	**67.8 ps**

Table 1: Beam timing detectors and t_0 resolutions for five different runs and beam momenta.

arrival time of the beam particle at the target region. This calculated value acts as a t_0 for subsequent secondary time-of-flight measurements.

The resolution on ToFA/TofB time-of-flight is ≈ 170 ps and only slightly worse for time differences that include the TDS counter. Individual detector resolutions can be determined using the time-of-flight resolutions of the pair-wise time-differences.

Using the fact that the uncertainty on the momentum is negligible compared to the time measurements t_0 can be found from the average of three independent t_0 values, each with the uncertainty of their respective time measurement, σ_{t_i}. For a sample whose individual measurements have independent uncertainties, the error on the mean can be found from the weighted average. Table 1 lists the t_0 resolutions for five runs.

As stated above, the calculated t_0 acts as the start time for secondary particle time-of-flight measurements. The resolutions of the pion and proton peaks are 180.4 ps and 185.7 ps, respectively.

3.2 Further developments on PID with the TOF-wall

Roughly 12% of the tracks hit the overlap region of the TOF wall detectors. For those tracks two independent time-measurements are available. The improved resolution is shown in Fig. 5. This feature is of particular importance for the MiniBooNE experiment, where one of the main backgrounds is generated by kaon-decays into electron-neutrinos.

Kaons and pions are well separated at 3σ up to 3 GeV/c momentum, the full relevant region for MiniBooNE and K2K, as shown in Fig. 5. The K/p separation extends up to 5 GeV/c for these tracks.

4 Large Angle Detectors

A brief report of the status of the TPC performance was given at the Siena conference. The contribution to the proceedings is reproduced in the Appendix. It is shown that the calibration is now far advanced. A lot of valuable information was obtained with the TPC-calibration campaign in summer 2003 using cosmic rays. In particular, the following results were obtained:

- A calibration with a ^{55}Fe and ^{83}Kr sources was performed. The Fe source has the advantage of delivering pad-charges more similar to particle tracks in the TPC. The comparison of the Fe and Kr data allows a comparison of the calibration constants at different ranges of pulse-heights to be made, and hence provides a check of the linearity of the response.

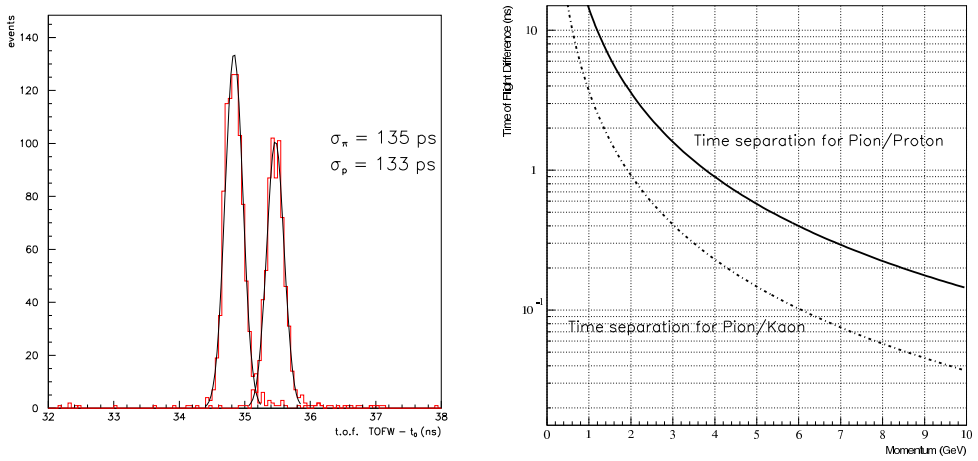

Figure 5: Left panel: Resolution of the overall TOF for pions and protons in an exposure of 5 GeV/c empty target beam particles, for tracks in the overlap region of two scintillators in the TOF wall. Right panel: TOF separation for π, K and p in HARP.

- A scintillator rod inserted in the central field cage provided a trigger signal for cosmic rays which pass through the centre of the TPC. These data are of invaluable importance to study the momentum resolution and electrostatic distortions.
- The voltage applied to the inner field cage was varied in order to better study the effect on the distortions.
- The cross-talk effects were fully modelled in the simulation and a correction for the data was developed.

Most results are presented in the Siena contribution. We just reproduce here the presently achieved momentum and dE/dx-resolution (Fig. 6). For these results corrections for cross-talk were not yet implemented.

Since the developments of the correction for the cross-talk effects and the study of the distortions were not presented at Siena, these will be given in the following section. In the previous status report several methods to correct the cross-talk were described. Here we only report on the most complete mathematical description [14]. The method based on this model [15] was determined to have the best performance.

4.1 Correction for cross-talk effects

As previously reported [9] the TPC front-end electronics suffers from a cross-talk problem caused by capacitive couplings between the outputs of some preamplifiers and the inputs of other preamplifiers. It was found that the induced cross-talk signals could be predicted using the Fourier transforms of the signal from the pad inducing the cross-talk signal and the transfer function of the pad on which the cross-talk was induced, along with the capacitive coupling between the two pads (the FFT model) [14]. A series of measurements was taken to allow the determination of all parameters needed to fully describe the problem using this model, namely the transfer functions of each pad, a map of cross-talk relations and the capacitive couplings between such pads (see [9, 14] for details).

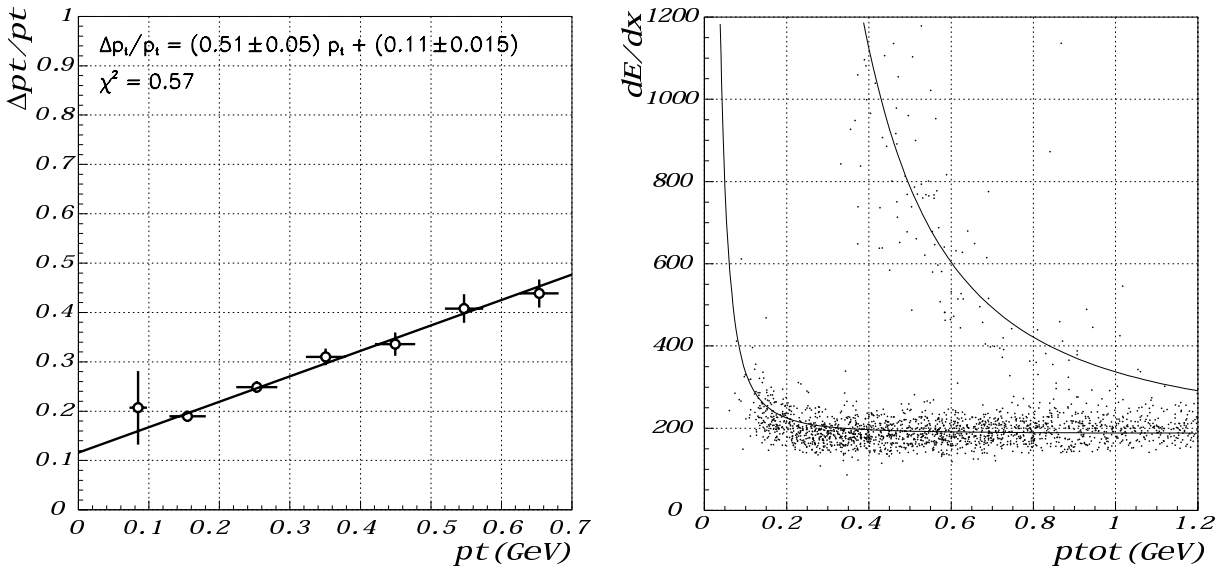

Figure 6: On the left the momentum resolution and on the right the dE/dx for the cosmic data taking in 2003. The two curves in the right hand panel indicate the expected response for pions (left curve) and protons (right).

Together, the model and these measurements allowed the cross-talk to be modelled in the Monte Carlo [15]. Initially this was done using the information from sector 6 to model the effect in each of the sectors. A detailed study to determine the effect of cross-talk on each stage of the reconstruction was carried out. Single track events with track inclinations of 80°, 60° and 40° were studied. It was found that cross-talk causes an increase in $r\phi$ residuals of around 25% and an increase in z residuals of 20–40%, as well as causing a large asymmetric shoulder in the z residual distribution. This results in a decrease in the number of points found by the pattern recognition of 8–18%, despite an increase in the number of points created per event of 5–10%. The result of these changes is a decrease in momentum resolution in both transverse and longitudinal directions.

The Monte Carlo has been utilised to design a correction based on the FFT model. The signal shapes are corrected by predicting the cross-talk signals using the FFT model and subtracting these predicted cross-talk signals from the signals measured, since the measured signals are the summation of the physics and cross-talk signals. Since the HARP TPC only records positive signals, any signals for which the negative swing of the cross-talk signal results in a negative portion of the final signal cannot be fully corrected since the negative part of the signal is lost. In such cases additional methods have to be employed to recover the signal (see [15] for more details on the correction method). The principle of this signal shape correction can be seen in Figure 7 which shows the correction process on a signal from a cosmic-ray event.

Signals for which too much information has been lost because too large an amount of the signal was negative and therefore not recorded cannot be corrected. Since not all signals can be corrected it is necessary to use additional methods in the reconstruction chain, to make the optimal use of the information gained from the correction of signal shapes. These consist of using only corrected signal shapes to reconstruct the position in $r\phi$ and z whenever possible, calculation of $r\phi$ position using a Gaussian fit rather than weighted mean of hits and the weighting of points in the fit according to how many pads are in the cluster and how many of these could be corrected.

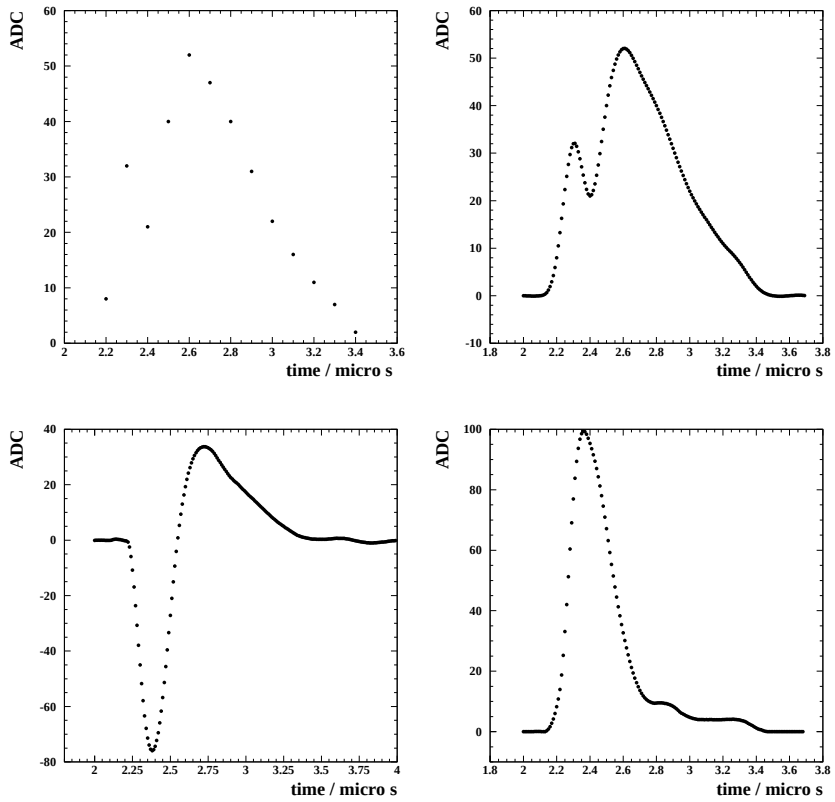

Figure 7: Example of a corrected signal shape from data. Shown are: original ADC series (top left), spline fit to ADC series (top right), predicted cross-talk signal (bottom left), corrected signal, which is the original signal with the cross-talk signal subtracted (bottom right).

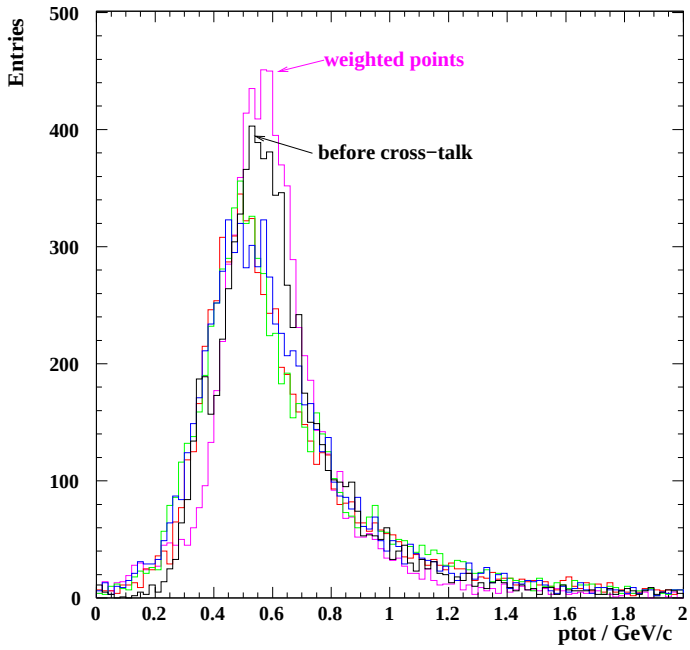

Figure 8: The distributions of total momentum for different cases: before cross-talk (black), cross talk (red), corrected ADC series (green), Gaussian fit of points (blue) and weighted points (magenta). The black and magenta histograms are labeled in the plot. After the cross-talk correction, the fit using weights assigned according to the quality of the information of the pads recovers the resolution.

The effect of the correction has been studied using both Monte Carlo and data. Comparisons with Monte Carlo truth show that improvements in $r\phi$ and z residuals, along with the weighting of points in the fit, allow the initial momentum resolution to be recovered (see Figure 8). Studies using both cosmic-ray data taken during 2003 and a simulated cosmic-ray sample show a decrease in $r\phi$ residuals of 24 % in data and 13 % for Monte Carlo (see Figure 9). For z residuals the decrease is 16 % for data and 31 % for Monte Carlo; the asymmetric tail is also seen largely to disappear (see Figure 10). The results both demonstrate that the correction works well on the data and give further validation to the FFT model.

All results described above use only the data from sector 6 for which the data from pulser runs has been analysed to give the transfer functions, cross-talk relations and capacitive couplings. This analysis has now been completed for the other five sectors, and a study of differences of the effect of correction between sectors is currently being performed. So far the focus of work on cross-talk has been on the effect and correction of position and momentum measurements. Now that this has been shown to work successfully, work is underway to study the effects of cross-talk and its correction on energy resolution.

4.2 Distortion effects

Distortion effects were studied in the 2003 cosmic-ray run by varying the HV on the inner field cage. For a cosmic-ray track passing through the trigger scintillator in the center of the TPC, the effect of the distortions is to worsen the matching of the two halves of the track. The parameter D measures the matching distance defined as the difference of the reconstructed position at the first pad-row of the half-track and the predicted position using the full cosmic-ray track.

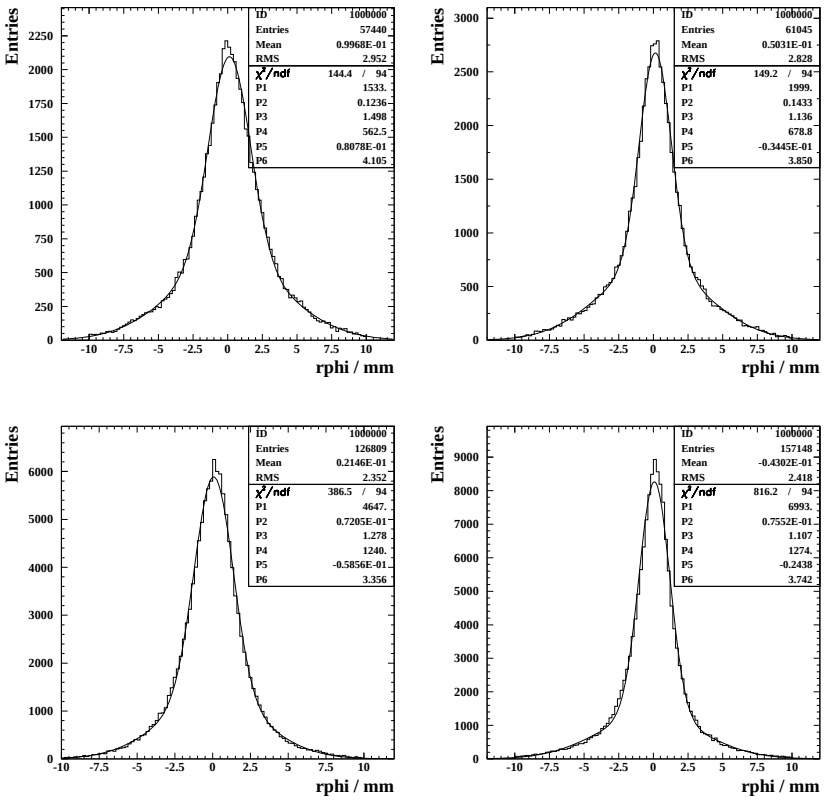

Figure 9: $r\phi$ residuals. For data (top) and Monte Carlo (bottom). Uncorrected measurements are shown on the left, and corrected ones on the right.

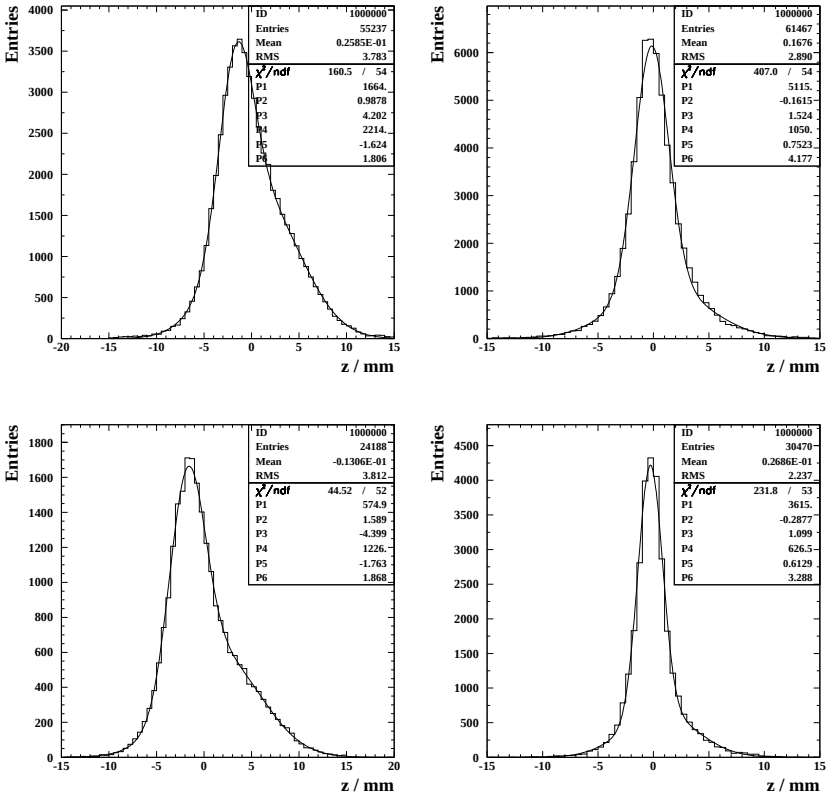

Figure 10: z residuals. For data (top) and Monte Carlo (bottom). Uncorrected measurements are shown on the left, and corrected ones on the right.

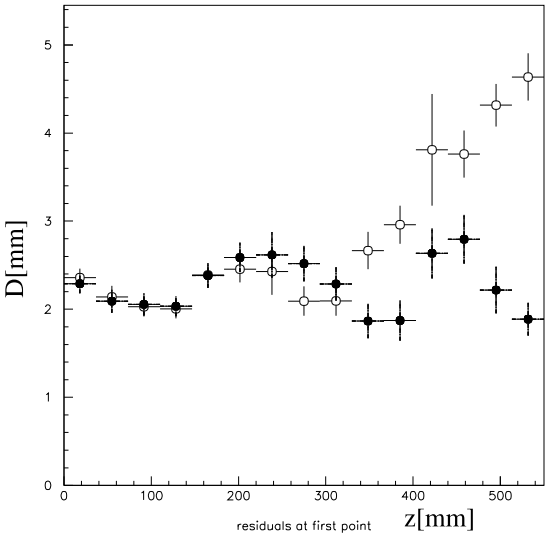

Figure 11: Improvement of D for the nominal voltage setting after distortion corrections. Original displacement (open circles), corrected (full circles).

A preliminary implementation of a simplified model for the distortions corrects most of the effect, as shown as function of z-position in Fig. 11. A correction based on a more complete electrostatic model is being developed.

4.3 Analysis of elastic scattering

Elastic scattering events in the data taken with the hydrogen target provide an interesting tool for the study of the performance of the TPC. In the absence of Fermi-motion, the kinematics is uniquely determined. The kinematical constraints can be used to study momentum resolution in the TPC, as well as in the forward spectrometer, energy deposition and other issues. The measurement of the rate provides a cross-check for total cross-section measurements.

Events were selected with a single track in the TPC emerging from the target in the 3 GeV/c beam. As shown in Fig. 12, this cut is sufficient to display a clear mass-peak. Selecting incoming pions or protons, the mass peak is seen at the position expected for the particle leaving the TPC in the forward direction. A further selection retaining only tracks in the TPC with a large energy deposition reduces the background, but leaves the peaks. Indeed, it is expected that the large-angle particle is a proton in this process.

4.4 RPCs

The work on the calibration of the RPC system has not yet given a satisfactory result. This effort is being reorganised. The committee will be informed of the progress as soon as possible.

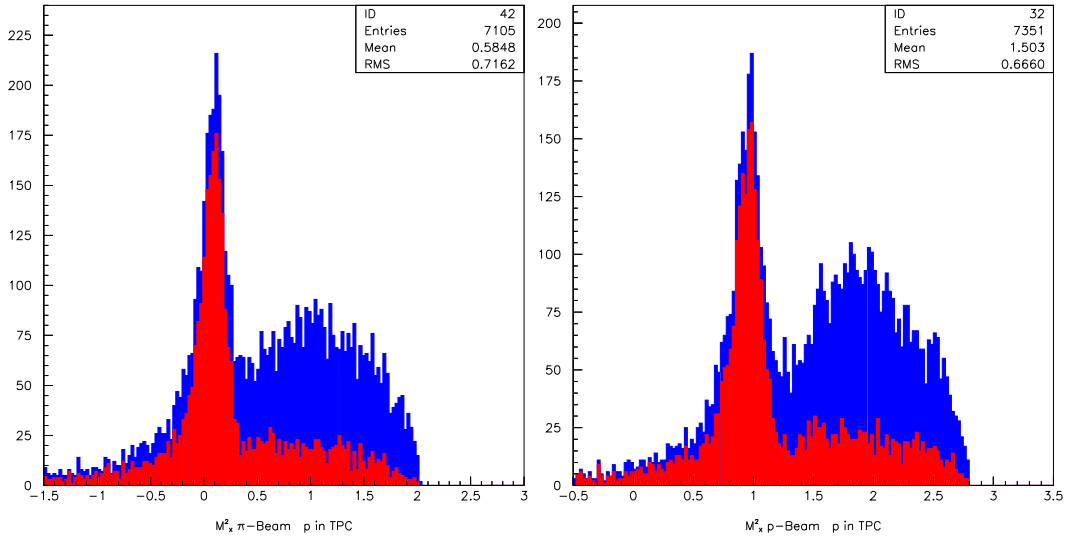

Figure 12: Missing mass distribution (m^2) selecting events with a single track in the TPC emerging from the target (blue/dark histogram) and with an additional selection on dE/dx to select tracks with a large energy-deposition (red/lighter histogram). On the left with incoming pions, on the right with incoming protons.

5 Software

Since the previous status report the major technical developments were concerned with creating the capability to store the result of the reconstruction for high-statistics analyses and to allow HARP collaborators to analyse data outside CERN.

The main developments were:

- The migration from Objectivity to Oracle as persistency solution for the raw data was completed. This project was done in close collaboration with Andrea Valassi (IT). The transition occurred without negative impact on the users.
- The concept of "intermediate DSTs" (*iDSTs*) was introduced. The iDST contains all reconstructed objects needed to perform the analysis and allows re-running of the reconstruction algorithms. The persistency solution is either ASCII files or a mySQL database. The size of the data is reduced by an order of magnitude compared to the raw data. iDSTs were used as the basis of the Moriond analysis.
- MiniDSTs were introduced to enhance the high-statistics capability. These contain high-level objects to be used as a basis for the final analysis. The persistency is compatible with the ASCII solution for the iDSTs. The data volume is reduced by another order of magnitude with respect to the iDSTs.

  By design it is not possible to re-run the reconstruction algorithms starting from the miniDST. The implementation of the miniDST is framework-neutral; the miniDSTs can be read with Gaudi as well as other analysis frameworks.
- Work is advanced on the full DSTs, which contain the same information as the iDSTs, but reside in ORACLE and contain in addition the meta-data needed to perform complete

productions automatically. It is the intention that iDSTs can be extracted from the DSTs for use outside CERN without processing overheads.

The iDSTs and miniDSTs are fully portable. Users outside CERN can analyse HARP data using these files, and an analysis release is available allowing the installation of all necessary software (including external libraries) anywhere.

6 Conclusions

At the previous status report it was shown that the calibrations for all detectors forming the forward spectrometer were of sufficient quality to enable analysis of the data. Indeed, first results on pion yields for K2K could be presented at conferences. High efficiency has been achieved for the tracking in the forward spectrometer with a good momentum resolution. The PID is capable of cleanly separating electrons, pions and protons in the relevant momentum range. A number of missing elements needs to be completed before a reliable final analysis can be presented. We estimate that this analysis will be completed in two months. Work on the MiniBooNE data has started.

Also the software tools were further developed to allow a high-statistics analysis of the complete data-set to be performed.

For the large-angle spectrometer, all effects have been studied and the understanding of the calibration and performance of the TPC is now far enough advanced that physics analysis can be started still by this summer. The results of the TPC-calibration campaign performed in 2003 with cosmic rays have permitted a better understanding of the energy-deposition response, momentum resolution and the electrostatic distortions. An algorithm to correct for the cross-talk is operational. A full simulation describing the performance of the TPC is available.

Acknowledgements

We wish to thank the IT/DB group of the IT Division at CERN and personally Andrea Valassi for designing and executing the migration of the HARP data and software from Objectivity to the new storage system based on Oracle. We would also like to thank the IT/ADC and IT/DS groups for contributing to the setup of the migration infrastructure and allocating the relevant hardware resources and the PH-EP-TA1 group for support during the TPC calibration campaign.

References

[1] M. Anfreville *et al.*, Nucl. Instr. and Meth. A481 (2002) 339.

[2] M. Baldo-Ceolin et al. ,*"The time-of-flight TOFW detector of the HARP experiment: construction and performance"*, 2004, to by published in Nucl. Instr. and Meth.

[3] G. Barichello et al., *"The HARP TOF-WALL counter construction and test"*, INFN-AE-02-01, HARP-MEMO-02-001.

[4] The CHORUS Collaboration, Nucl. Instr. and Meth. A349 (1994) pp.70-80.
The CHORUS Collaboration, Nucl. Instr. and Meth. A378 (1996) pp.221-232.

[5] G. Prior, Nucl.Phys. B (Proc. Suppl.) 125C pp.37-42

[6] M. Bogomilov et al., *"The HARP RPC time-of-flight system"*, Nucl. Instr. and Meth. A508(2003)152-158.

[7] I. Stancu *et al.* MiniBooNE collaboration, *"The MiniBooNE Detector Technical Design Report"*, FERMILAB-TM-2207.

[8] M. H. Ahn *et al.* K2K Collaboration, *"Indications of neutrino oscillation in a 250-km long-baseline experiment"*, Phys. Rev. Lett. 90 (2003) 041801.

[9] The HARP collaboration, CERN-SPSC/2003-027.

[10] A. Cervera, HARP coll., Proceedings, Rencontre de Moriond 2004.

[11] S. Borghi, HARP coll., Proceedings, IPRD04, Siena 2004.

[12] G. D'Agostini, Nucl. Instrum. Meth. A362 (1995) 487.

[13] A. Grossheim, *"Particle production yields induced by multi-GeV protons on nuclear targets"*, PhD. Thesis, University of Dortmund, 2004.

[14] G. Vidal Sitjes, *"The HARP Time Projection Chamber"*, PhD. Thesis, Universidad de Valencia, 2003.

[15] L. Howlett, *"Simulation and Correction of Cross Talk in the HARP Time Projection Chamber"*, PhD. Thesis, University of Sheffield, 2004.

A Appendices